

# The Use of a Wave Prediction Model for Driving a Near-Surface Current Model

Alastair D. Jenkins

UDC 551.465.11:551.465.5

## Summary

The current near the sea surface is an important influence on the drift and dispersion of plankton, fish eggs and larvæ and other marine organisms, of oil slicks, chemical pollutants and other substances, and contributes significantly to the forces on marine structures. Since it is intimately associated with air-sea momentum and energy transfer, it affects, and is affected by, the atmospheric conditions, and, in the long term, the global climate.

Since surface gravity waves are almost always present at the air-sea interface, and carry significant energy and momentum, they should be taken into account when estimating near-surface currents. A one-dimensional current model is presented which does take waves into account. It uses a Lagrangian coordinate system, and the source terms from a directional spectral wave prediction model act to transfer momentum from the wave field to the current. After the wave model is run, but before it is used to drive the current, the source terms in the tail of the wave spectrum are parameterized in a way which deals consistently with the balance of wave energy, momentum and action. Numerical integration is performed by using a finite difference grid with a fine resolution near the surface, and an implicit time-stepping scheme is used. The model results are consistent with present knowledge of the behaviour of the surface current. Within the upper 1 metre, they depend strongly upon the behaviour of the wave spectral tail. Oscillations in the modelled high-frequency wave components, which arise when the wind forcing is changed rapidly, give rise to corresponding oscillations in the current: this effect may be physical or it may be due to a slight instability in the wave model.

## Die Verwendung eines Wellen-Vorhersagemodells für das Betreiben eines Modells oberflächennaher Strömungen (Zusammenfassung)

Die oberflächennahe Strömung im Meer hat einen bedeutenden Einfluß auf die Drift und Ausbreitung von Plankton, Fischeiern, Larven und anderen marinen Organismen, von Ölflecken, chemischen Schadstoffen und anderen Substanzen und liefert den Hauptbeitrag der Kräfte, die auf marine Bauwerke einwirken. Da sie eng verknüpft sind mit dem Impuls- und Energietransfer zwischen Ozean und Atmosphäre, beeinflussen sie den Zustand der Atmosphäre und langfristig betrachtet das globale Klima, bzw. werden dadurch beeinflusst.

Da Schwerewellen an der Grenzfläche Luft–Wasser fast ständig vorhanden sind und Energie und Impuls transportieren, sollten sie bei der Abschätzung oberflächennaher Strömungen berücksichtigt werden. In dieser Arbeit wird ein eindimensionales Strömungsmodell vorgestellt, das den Einfluß von Wellen berücksichtigt. Das Modell rechnet in einem Lagrangeschen Koordinatensystem. Die Quellterme, die aus einem Vorhersagemodell für das Richtungsspektrum des Seegangs stammen, bewirken den Impulstransfer vom Wellenfeld zur Strömung. Nach dem Lauf des Wellenmodells werden die Quellterme im hochfrequenten Ende des Spektrums

parametrisiert, bevor sie in das Strömungsmodell eingehen. Diese Parametrisierung ist konsistent mit dem Gleichgewicht der Wellenenergie, des Wellenimpulses und der Wellenwirkung. Die numerische Integration geschieht in einem zeitlich impliziten Differenzenverfahren mit einem Gitternetz, das in Oberflächennähe eine feinere Auflösung hat. Die Modellergebnisse sind in Übereinstimmung mit dem gegenwärtigen Kenntnisstand über das Verhalten der Oberflächenströmungen. Innerhalb des ersten oberen Meters hängen die Ergebnisse stark vom Verhalten des hochfrequenten Endes des Wellenspektrums ab. Schwingungen in der modellierten hochfrequenten Wellenkomponente, die bei einer abrupten Änderung der Windanregung auftreten, lassen korrespondierende Schwingungen in der Strömung anwachsen: Dieser Effekt könnte physikalischer Natur sein oder aus einer schwachen Instabilität des Wellenmodells herrühren.

### **L'utilisation d'un modèle de prévision de vague pour forcer un modèle de courant superficiel (Résumé)**

Le courant superficiel a une influence importante sur la dérive et la dispersion du plancton, des oeufs de poisson, des larves et autres organismes marins, sur celles des nappes de pétrole, des polluants chimiques et d'autres substances. Il contribue de façon significative aux forces qui agissent sur les structures marines. Puisque ce courant est intimement lié aux interactions air–mer il affecte et est affecté par les conditions atmosphériques et à long terme le climat.

Comme les ondes de gravité qui sont presque toujours présentes à l'interface air–mer transportent une énergie et une quantité de mouvement significatives, elles devraient être prises en compte lorsqu'on veut faire une estimation des courants superficiels. Ainsi est présenté un modèle unidimensionnel de courant prenant en compte ces ondes. Il utilise un système de coordonnées Lagrangien et les résultats d'un modèle spectral de prédiction de direction des vagues pour transférer la quantité de mouvement du champ de vague au courant. Après avoir fait tourner le modèle de vague, mais avant d'en utiliser les résultats pour modéliser le courant, les résultats obtenus pour l'extrémité du spectre de vagues sont paramétrés d'une façon qui respecte l'équilibre de l'énergie et de la quantité de mouvement des vagues avec le mouvement.

L'intégration numérique est obtenue à partir d'une grille aux différences finies avec une fine résolution près de la surface et d'un schéma implicite pour le pas de temps. Les résultats du modèle sont cohérents avec la connaissance actuelle du comportement des courants de surface.

Dans la couche 0–1 mètre, ils sont très sensibles au comportement de l'extrémité du spectre des vagues.

Les variations des composantes à haute fréquence des vagues qui apparaissent dans le modèle lorsque le forçage du vent change rapidement donnent lieu à des variations correspondantes du courant.

Cet effet peut être physique ou peut être dû à une légère instabilité du modèle de vague.

## **1 Introduction**

The current near the sea surface is an important oceanographic parameter. It contributes to the environmental loading on fixed and floating offshore structures, as an addition to the wave forcing; it affects the dispersion, drift and spreading of oil and other pollutants on or near the sea surface; it influences various biological processes, such as the drift of fish eggs and larvæ. On medium to long time scales, it can also be expected to have some

influence on the weather and climate, as well as on the circulation of the deeper ocean, in conjunction with other physical processes occurring near the sea surface (e.g., turbulence, surface waves), since the surface of the sea is the interface between the ocean and the atmosphere.

Ekman [1905] demonstrated the profound effect of the rotation of the Earth on the vertical current structure. If the vertical transport of momentum, by turbulent mixing etc., can be described by an “eddy viscosity”,  $\nu$ , the direct shearing effect of the wind is limited to a depth of order  $(2\nu/|f|)^{1/2}$ , where  $|f|$  is the Coriolis parameter, although significant effects in the interior can be generated by horizontal variations in the wind forcing causing vertical water movements (“Ekman pumping”) via the continuity equation (e.g., Gill [1982]). If the eddy viscosity is assumed to be constant, the current will tend to evolve towards a steady state in which, in the northern hemisphere, the surface current is directed at  $45^\circ$  to the right of the wind direction, and the current decreases exponentially and rotates clockwise with increasing depth. However, field observations of surface drift currents, reviewed by Huang [1979], indicate that the angle between wind and current is much smaller, generally about  $10^\circ$ . Such small angular deviations can be reproduced if we use a vertically varying eddy viscosity in the ocean which is very small at the sea surface and increases rapidly with increasing distance from the surface (e.g., Madsen [1977]). Even if a constant eddy viscosity is used, the angle between wind and current is reduced from the  $45^\circ$  value if the effect of wind-generated surface waves is included (Weber [1983a]).

In this paper I will pay particular attention to the effects of surface waves, since waves are almost invariably present at the sea surface and carry with them very significant concentrations of both kinetic and potential energy, transporting such energy horizontally with speeds (wave group velocities) greatly in excess of those of typical ocean currents. They cause water particles to drift, even in the absence of other fluid movements, since particle orbits are not closed in irrotational waves (Stokes [1847]). Waves can also be thought of as having momentum (or at least a momentum *flux*, so that momentum is transported at the wave group speed, see McIntyre [1981]). The rate of momentum transfer between the atmosphere and the ocean, given by the “wind stress”, depends on the surface roughness, which can in turn be affected by the surface wave field (Kitajgorodskij [1973]). Wave breaking (whitecapping) and other forms of wave energy dissipation inject substantial amounts of turbulent kinetic energy, and also air bubbles, into the near-surface ocean, contributing to oceanic mixing and air-sea gas transfer (Thorpe [1985]). Other contributions to near-surface mixing include Langmuir circulations, probable mechanisms for which include instabilities in the wind and wave induced current field (Leibovich and Paolucci [1981]). Present-day techniques for the numerical simulation of vertical current structure, using an eddy viscosity for vertical momentum transfer (e.g., Backhaus [1985]; Davies [1986]), are able to produce fairly good results. However, as more powerful computers are becoming available, there has been an increasing interest in improving modelling results by investigating better representations of dynamical processes, such as turbulent energy balance (e.g., Davies and Jones [1987]) and wave-dependent drag coefficient dependence (Wolf, Hubbert and Flather [1988]). The model described in this paper addresses a third process: the balance of wave momentum.

Surface waves can propagate energy over considerable distances. Snodgrass, Groves, Hasselmann et al. [1966], in a detailed observational study of swell propagation in the Pacific Ocean, observed swell at Honolulu from a storm near Madagascar – an angular distance of nearly  $170^\circ$ . Storms near Newfoundland have been observed to generate swell with a wave height of several metres near the Norwegian coast (Gjevik, Krogstad, Lygre and Rygg [1988]). It is reasonable to suppose that waves can also transfer momentum in a similar fashion, so that the effect of wind forcing at one place will act on the ocean a considerable distance away. Longshore drift is an example of this phenomenon – the along-shore component of the momentum flux of waves which dissipate on a coast generates a current along the coast (Longuet-Higgins [1970]) – and since wave



dissipation, by whitecapping, for example, also occurs in the open sea, we can expect waves to influence the current away from coastal boundaries as well. To model the effect of waves on the current, it is necessary to have a representation of the wave field. This can be done either empirically (e.g., by specifying the waves as some function of the wind velocity) or by using some kind of wave model. There are many models now available for calculating ocean waves (The SWAMP Group [1985]), some of which use "rule-of-thumb" techniques, and others which attempt a more consistent representation of the physical processes involved.

## 2 Description of the surface wave field

### 2.1 Introduction

The simplest description of surface waves is as a single sine wave component with a given wave height, frequency, wavelength and direction. However, the ocean surface is easily seen to be very irregular, and can much better be described by a superposition of many sine wave components with different frequencies and directions. It is often convenient to assume that the wave field can be represented as a linear Gaussian random process with a specific dispersion relation between frequency and wavelength. Before we write down explicit formulæ for such a representation, however, I would like to make a digression, to discuss the coordinate system which I will use.

### 2.2 Coordinate system

Formulæ and equations of fluid dynamics are usually written in an Eulerian formulation where the velocity, density and other properties of the fluid are functions of the ordinary Cartesian coordinates  $(x, y, z)$ . This formulation has disadvantages when a free surface is present, since points which have vertical coordinates  $z$  between wave trough and wave crest are sometimes within the water and sometimes in the air. It is then difficult to define mean properties, such as the current, for such points. This difficulty can be avoided for waves of fixed form by choosing a curvilinear coordinate system which moves with the waves, as was done by Longuet-Higgins [1953], but such a coordinate system will also need to have time-dependent deformations if a random wave field is to be described.

For this reason, I have chosen to use a "Lagrangian" formulation, in which the properties of the fluid, including the ordinary Cartesian components of the actual positions,  $\mathbf{x} = (x, y, z)$ , and velocities,  $\mathbf{u} = (u, v, w)$ , of fluid particles, are represented as functions of the  $t$  and spatial coordinates  $(a, b, c)$  which are fixed with respect to the fluid particles, and where the instantaneous sea surface is represented by  $c = 0$ . This Lagrangian representation allows us to look at variations in water properties very near the sea surface: for example vertical variations in the mean velocity (drift current) at distances from the surface much smaller than the vertical excursion of the surface due to wave motion. A true Lagrangian coordinate system can be difficult to deal with, since the presence of a sheared mean drift current will produce greater and greater distortions of the coordinate system as time goes on: this difficulty can be avoided, as was done by Andrews and McIntyre [1978], by choosing a coordinate system which follows the wave motions but which does not drift or distort with the mean current. A less rigorous viewpoint, used in this paper, is to employ a true Lagrangian coordinate system but to ignore its long-term distortion, assuming, in effect, that we can obtain sufficient information about the system by analysing it over a relatively short period, during which the distortion of the coordinates does not become too great.

Fig. 1 shows the coordinate system used, the distortion of the grid being due to a wave which moves fluid particles  $(a, b, c)$  to the positions  $(a + \xi, b, c + \zeta)$  in Cartesian coordinates, where  $\xi$  and  $\zeta$  are sinusoidal functions of  $a$  and  $t$ . Waves of this form were

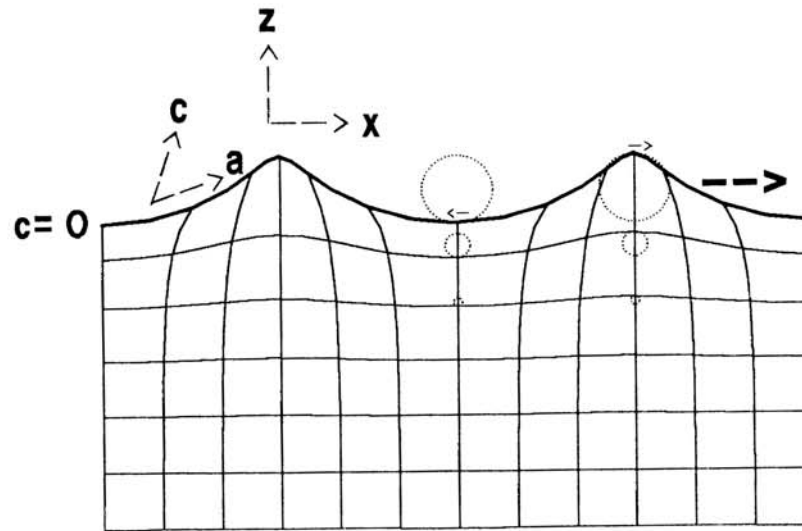


Fig. 1 An example of the coordinate system used, for a single sinusoidally-oscillating wave, propagating towards the right in the  $xz$  plane.  $x$  and  $z$  are Cartesian coordinates,  $a$  and  $c$  are the Lagrangian coordinates – the grid shows lines of constant  $a$  and  $c$ , with  $c = 0$  at the water surface. The dotted circles show water particle orbits, the small arrows indicating the direction of water movement

described by Gerstner [1804], and satisfy the equations of motion exactly for an inviscid fluid. They are, however, rotational, having a vorticity of order  $\epsilon^2$  ( $\epsilon = k\zeta_0$  is the wave slope,  $k$  being the wavenumber and  $\zeta_0$  the wave amplitude), and so cannot be set up by surface forces from an initial state of rest in an inviscid fluid. However, an irrotational wave field in an inviscid fluid will, in fact, under the influence of Coriolis forces, change to become the sum of a near-Gerstner wave and an inertial oscillation within a quarter of an inertial period (Ursell [1950], Pollard [1970]).

### 2.3 Explicit formulæ for a random wave field

We denote the displacement of fluid particles from their reference position  $\mathbf{y} = (a, b, c)$  by  $\xi = (\xi, \eta, \zeta)$ , so that their actual position is  $\mathbf{x} = \mathbf{y} + \xi$ . We assume, to  $O(\epsilon)$ , that the particle displacements can be described by superimposing linear, deep-water Gerstner-type waves, so that

$$(\xi, \eta, \zeta) = \text{Re} \int_{f=0}^{\infty} \int_{\theta=0}^{2\pi} \left( i \cos \left( \frac{\pi}{2} - \theta \right), i \sin \left( \frac{\pi}{2} - \theta \right), 1 \right) \exp [i(\mathbf{k} \cdot \mathbf{y} - 2\pi f t)] \times \exp(kc) dZ(f, \theta), \quad (1)$$

where the wavenumber vector  $\mathbf{k} = k\hat{\mathbf{k}}$ ,  $k = 4\pi^2 f^2/g$ ,  $\hat{\mathbf{k}} = (\cos(\frac{\pi}{2} - \theta), \sin(\frac{\pi}{2} - \theta), 0)$ ,  $g$  is the acceleration due to gravity,  $f$  is the wave frequency and  $\theta$  is the direction of the wave vector, measured clockwise from “northward”.  $Z$  is a random function—strictly speaking, a *measure* (Barstow and Krogstad [1984])—with orthogonal increments, so that

$$E[dZ^*(f', \theta') dZ(f, \theta)] = \begin{cases} 2 F(f, \theta) df d\theta, & f = f' \text{ and } \theta = \theta', \\ 0, & \text{otherwise,} \end{cases} \quad (2)$$

where the asterisk denotes complex conjugation,  $E[\cdot]$  denotes the mathematical expectation, and  $F(f, \theta)$  is the “directional wave spectrum”, which, when integrated over all frequencies and directions, gives the variance of sea-surface elevation:

$$E[\zeta^2|_{c=0}] = \int_0^\infty df \int_0^{2\pi} d\theta F(f, \theta). \quad (3)$$

The total wave energy per unit area is equal to  $\rho g E[\zeta^2|_{c=0}]$ , where  $\rho$  is the water density.

This description of the wave field requires, strictly speaking, a spectrum  $F$  which does not vary in space or time. For practical purposes, this condition can be relaxed somewhat, allowing variations which are on long space and time scales with respect to wave period and wavelength. We can write down an expression for the evolution of the wave spectrum:

$$\frac{\partial F(f, \theta)}{\partial t} + \mathbf{v}_g(f, \theta) \cdot \nabla F(f, \theta) = S_{in}(f, \theta) + S_{nl}(f, \theta) + S_{ds}(f, \theta), \quad (4)$$

where  $\mathbf{v}_g$  is the group velocity of the appropriate wave component and the  $S$  terms denote contributions to the total rate of change of the energy (variance) of each wave component, which can be specified by theory, experiment or empirical expressions.  $S_{in}$  is the rate of energy input from the atmosphere,  $S_{nl}$  is the contribution from components of different wavenumbers by non-linear wave-wave interaction, and  $S_{ds}$ , which is always negative, represents wave energy dissipation and includes contributions from wave breaking, turbulent dissipation, and so on.

The total wave momentum per unit area,  $\mathbf{p}_{tot}$ , is given by the vertically integrated Stokes drift:

$$\mathbf{p}_{tot} = \rho \int_{-D}^0 \mathbf{u}_s(c) dc, \quad (5)$$

where  $D$  is the total depth, and, for  $D \gg (2k)^{-1}$ ,

$$\mathbf{u}_s = 4\pi \iint f \mathbf{k} e^{2kc} F(f, \theta) df d\theta. \quad (6)$$

The nonlinear interaction term,  $S_{nl}$ , can be calculated by  $O(\epsilon^3)$  perturbation theory (Hasselmann [1962]), and conserves wave momentum as well as energy and wave action, when integrated over all frequencies and directions. In practice, approximate expressions are used for  $S_{nl}$ , since evaluation of the full  $O(\epsilon^3)$  expression requires very lengthy computations.

### 3 Model for surface currents

The wave field induces a mean flow of order  $\epsilon^2$ . For an inviscid fluid, in the absence of rotation, this is the Stokes drift. In a rotating frame, the Coriolis force turns this into wave-induced inertial oscillations (UrSELL [1959], Hasselmann [1970], Pollard [1970]). The presence of viscous forces within the fluid acts to damp the waves and also allows momentum to be transported vertically by shear stresses. A thin viscous boundary layer, with thickness of order  $(\nu/\pi f)^{1/2}$ , appears just near the water surface, and the mean drift velocity below this boundary layer is modified considerably, even for extremely small

viscosities (Longuet-Higgins [1953]). The effect of the Earth's rotation on wave-induced currents was considered by Weber [1983b], and the combined effect of wind and waves in a rotating frame by Weber [1983a] and Jenkins [1986]. Longuet-Higgins developed his theory using a curvilinear Eulerian coordinate system which moved with the waves, whereas Weber and Jenkins used a Lagrangian formulation, expanding the equations of motion to  $O(\epsilon^2)$ .

In the articles mentioned above, the (eddy) viscosity was assumed to be constant. The case of a vertically varying eddy viscosity was treated by Jenkins [1987a], who, in a subsequent paper (Jenkins [1987b]), indicated how the theory could be applied to the case of a random wave field, with the energy balance given by equation (4). The wave damping and the vertical transport of momentum within the current field are both determined by the same eddy viscosity profile, and a consequence of this is that the dissipation source term,  $S_{ds}$ , is equal to a weighted integral of the eddy viscosity with respect to the Lagrangian vertical coordinate,  $c$ .

If we apply the theory developed by Jenkins, using a wind stress  $\tau = \rho u_*^2$ , where  $u_*$  is the friction velocity in the water, and a wave field given by the theoretical fully-developed wind-sea spectrum of Komen, Hasselmann and Hasselmann [1984], the dissipation source function  $S_{ds}$  is reproduced with an eddy viscosity which is proportional to  $c$  with a vertical gradient of approximately  $-1.1 \times 10^{-2} u_*$ . However, a more "realistic" gradient of the eddy viscosity which transfers momentum between the current at different depths is given by the "law-of-the-wall" relation of Madsen [1977],  $\nu = -\kappa u_* c$ , with  $\kappa \approx 0.4$  being von Kármán's constant. The former value gives a very thin Ekman layer, and surface drift speeds considerably larger than expected from field observations of the drift of oil slicks etc. (Jenkins [1987c]). There is also a physical reason to suppose that the effective "current" eddy viscosity should be greater than the "wave" eddy viscosity: the Reynolds stresses which transfer momentum within the current profile include contributions from velocity fluctuations with time scales much greater than the wave period – Langmuir circulations, for example. The model equations which are presented below, therefore, although based on the second-order perturbation expansion of Jenkins [1987a, b], are modified to allow  $S_{ds}$  to be specified independently of  $\nu$ . They do, however, treat wave momentum in a consistent way – if waves dissipate, their momentum acts to accelerate the "non-Stokes drift" part of the current.

We consider the variation of the current in one dimension only (vertically), although we allow the wave field to vary slowly in the horizontal. Mean horizontal pressure gradients are ignored – their effect can just be added, if required, as the model equations are linear. The equations have a fairly simple form if we use what I call the "quasi-Eulerian" current,  $\mathbf{u}_E = \mathbf{u}_L - \mathbf{u}_s$ , ( $\mathbf{u}_L$  is the mean drift velocity or "Lagrangian mean current"), which corresponds to the " $\bar{\mathbf{u}}^L - \mathbf{p}$ " of Andrews and McIntyre [1978]. The eddy viscosity is assumed to be a function of  $c$  alone. The Coriolis acceleration is determined by the vertically-pointing vector  $\mathbf{f} = (0, 0, 2\Omega \sin \phi)$ , where  $\Omega$  is the Earth's angular velocity of rotation and  $\phi$  is the latitude.

The momentum equation is as follows:

$$\frac{\partial \mathbf{u}_E}{\partial t} + \mathbf{f} \times \mathbf{u}_E - \frac{\partial}{\partial c} \left( \nu \frac{\partial \mathbf{u}_E}{\partial c} \right) = -\mathbf{f} \times \mathbf{u}_s - 2\pi \int df \int d\theta f \hat{\mathbf{k}} S_{ds}(f, \theta) \quad (7)$$

$$\times 2kN(f, \theta; c) \exp(2kc)$$

The last term redistributes the momentum lost from the waves by dissipation. The function  $N(f, \theta; c)$  expresses the mechanism of the transfer of momentum from the wave field into the current, and is constrained by the following condition: for all  $f$  and  $\theta$ , the integral of  $2kN(f, \theta; c) \exp(2kc)$  through the whole depth is equal to unity. Otherwise, very little is known about this wave-current momentum transfer, and it can be argued that  $N$  could just



as well be a delta function at the sea surface. If the dissipative process is simulated by applying an eddy viscosity  $\nu_w$  which is independent of time and wavenumber but which can vary with  $c$ ,  $N$  becomes the sum of a delta function proportional to the surface value of  $\nu_w$  with a positive proportionality constant and a term proportional to  $\partial \nu_w / \partial c$  with a negative proportionality constant (J e n k i n s [1987a, c]).

In this paper, I use  $N = 1$ , which corresponds to a  $\nu_w$  which is zero at the surface and proportional to  $c$  below the surface.

The boundary condition at the sea surface is

$$\nu \frac{\partial \mathbf{u}_E}{\partial c} \bigg|_{c=0} = \frac{\tau}{\rho} - 2\pi \int df \int d\theta f \hat{\mathbf{k}} S_m(f, \theta), \quad (8)$$

where  $\tau$  is the wind stress vector.

Strictly speaking, equations (7) and (8) apply below the thin surface viscous boundary layer, but even within this layer the current will only change by a small factor, of order  $2k(\pi f/\nu)^{1/2}$ , though its vertical gradient will be altered by a factor of order unity.

The equations are solved using a finite difference method, with a grid size which varies with  $c$ , being very fine near the surface and coarser lower down. Because of the very fine grid, stability requires the use of implicit time-stepping. The Coriolis terms are evaluated as the average of their values at the present time step ( $t$ ) and the future time step ( $t + \Delta t$ ), and the viscous and forcing terms are evaluated at the future time step only. This means that the truncation error is  $O(\Delta t^2)$  for the Coriolis terms and  $O(\Delta t)$  for the viscous terms, but the lower-order accuracy is justifiable for the viscous terms, since "eddy viscosity" is not a precise concept. An  $O(\Delta t^2)$  approximation for the viscous terms can also give rise to spurious oscillations if large time steps are used (R o a c h e [1972]). At each time step, the presence of the Coriolis terms means that a linear system of equations with five diagonals has to be solved.

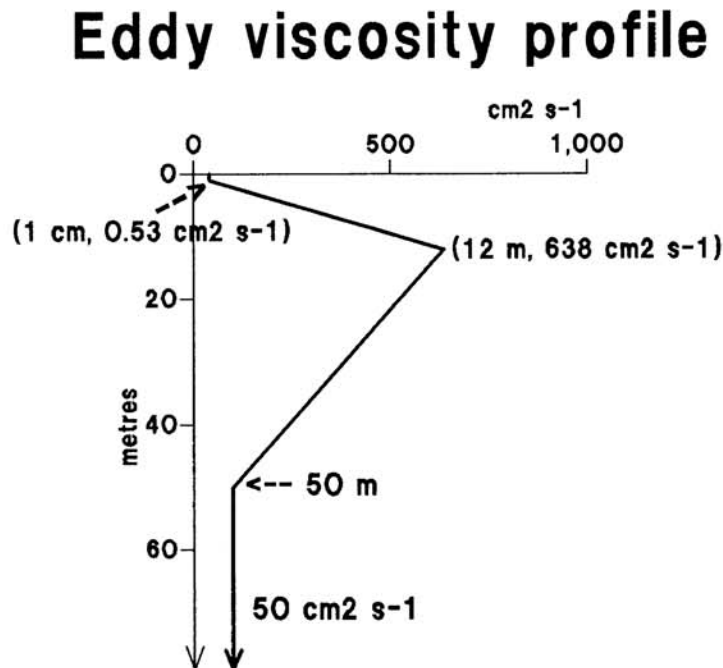


Fig. 2 The eddy viscosity profile used to transport momentum vertically within the current field (not to scale). This is a piecewise-linear approximation to the profile used by Weber [1981], incorporating Madsen's [1977] linear profile between 1 cm and 12 m depth



The model runs presented in this paper were with a grid of 200 points over a depth of 3000 metres (a reasonable approximation to infinite depth!), the grid size being  $\approx 5$  mm at the surface and  $\approx 30$  metres at the bottom. The time step was  $\approx 72$  seconds. It should be possible to use much larger time steps in practical applications, but it may be necessary to keep quite a fine grid near the surface to resolve the boundary layer. The Coriolis parameter,  $|f|$ , was set to  $1.21 \times 10^{-4} \text{ s}^{-1}$ , corresponding to a latitude of  $60^\circ \text{ N}$ , and a wind of  $10 \text{ m s}^{-1}$  was “switched on” over an ocean initially at rest, at  $t = 0$ . (The friction velocity in the air,  $U_* = (\rho/\rho_a)^{1/2} u_*$ , was set equal to  $0.3808 \text{ m s}^{-1}$ , where the air density  $\rho_a = \rho/800$ ). Fig. 2 shows the eddy viscosity profile which was used to transport momentum vertically within the current field – it is a piecewise-linear approximation to the profile used by Weber [1981], but has a constant value in the uppermost 1 cm, and incorporates, between 1 cm and 12 m depth, part of the linear profile,  $\nu = -0.4u_*c$ , used by Madsen [1977].

#### 4 Wave model

The wave forcing was specified by using a zero-dimensional (one point) version of the 3G-WAM spectral wave model (The WAMDI Group [1988]). This model calculates the wave spectrum  $F(f, \theta)$  for 12 directions in each of up to 25 logarithmically-spaced frequency bands, the ratio between adjacent frequencies being 1.1. The simulations presented here used a frequency range from  $\approx 0.06 \text{ Hz}$  to  $\approx 0.58 \text{ Hz}$ . In the main part of the wave spectrum, the source terms are calculated according to explicit formulae (see Komien et al. [1984]). The nonlinear interaction term  $S_{nl}$  is calculated using a “discrete-interaction” parameterization (Hasselmann, Hasselmann, Allender and Barnett [1985]).  $F(f, \theta)$  is made proportional to  $f^{-4}$  in the high-frequency tail of the spectrum, above 2.5 times the mean frequency or 4 times the Pierson-Moskowitz frequency,  $f_{PM} = g/(2\pi \cdot 28U_*)$ , whichever is the smaller. Since the high-frequency tail makes an important contribution to the momentum balance, I calculated “hypothetical” source terms for higher frequencies (up to the 60th frequency band, i.e., a frequency of  $\approx 28$  times that of the 25th band). Note that the behaviour of the wave field is unaffected by the source terms I calculated: they are used only to drive the current, via equations (7) and (8).

Firstly,  $S_{nl}$  was extended in such a way that it conserved wave energy, wave momentum, and wave action ( $\int \int f^{-1} F(f, \theta) df d\theta$ ), when integrated over the whole spectrum. An expression of the following form was used:

$$S_{nl}(f, \theta) = S_{nl}(f_{bm}, \theta) \left( \frac{f}{f_{bm}} \right)^{-6} \left[ 1 + A_1 \left( \frac{(f - f_{bm})}{f_{bm}} \right) + A_2 \left( \frac{(f - f_{bm})}{f_{bm}} \right)^2 + A_{2c} \left( \frac{(f - f_{bm})}{f_{bm}} \right)^2 \cos \theta + A_{2s} \left( \frac{(f - f_{bm})}{f_{bm}} \right)^2 \sin \theta + A_3 \left( \frac{(f - f_{bm})}{f_{bm}} \right)^3 \right], \quad f > f_{bm}, \quad (9)$$

where  $f_{bm}$  is the maximum frequency for which  $S_{nl}(f, \theta)$  is calculated directly.

This results in an underdetermined system of equations – 4 equations for 5 unknowns – for which the solution of minimum “length” ( $(= A_1^2 + A_2^2 + A_{2c}^2 + A_{2s}^2 + A_3^2)^{1/2}$ ) was found. A similar system of equations for 4 unknowns was found to be generally ill-conditioned.

After  $S_{nl}$  was determined,  $S_{in}$  and  $S_{ds}$  were adjusted so that  $S_{in} + S_{nl} + S_{ds}$  gave the wave model’s values for the rate of change of  $F(f, \theta)$ , for all  $f$  and  $\theta$ . This was, in fact, done for the whole spectrum, not just the tail, because sometimes the rate of change of  $F(f, \theta)$  was artificially “clamped” in the wave model to improve stability so that  $dF/dt$  was not always equal to the sum of the source terms calculated by the wave model.

## 5 Results

Fig. 3 shows the development of the Lagrangian mean current after a wind of  $10 \text{ m s}^{-1}$  is applied to an ocean initially at rest. Fig. 4 shows the corresponding quasi-Eulerian current, and Figs. 5 and 6 show time series of the  $x$ -components of the Lagrangian and quasi-Eulerian currents during the first 12 hours. The general behaviour of the current is similar to that predicted by other theories of the surface Ekman layer, with an initial rapid increase followed by slowly-damped inertial oscillations, the long-term mean current vector tracing out a spiral with increasing depth (e.g., E k m a n [1905], J e n k i n s [1986]). The small angular deviation of the surface current from the wind direction is typical of theories where the eddy viscosity near the surface increases with depth (e.g., M a d s e n [1977], J e n k i n s [1987 a]), and can still be seen if the waves are assumed to be absent (Fig. 7). The long-term surface mean drift current is rather high, just over 4% of the wind speed. This high value is probably due to the large surface Stokes drift values produced by a wave spectrum with an  $f^{-4}$  tail – if an  $f^{-5}$  tail is used, the mean surface drift is reduced to between 3% and 3.5% (Fig. 8), and if waves are ignored entirely, it is further reduced, to about 2.7% of the wind speed. From Fig. 9 we see that the simulation with the  $f^{-4}$  tail gives a Stokes drift at the surface of over 2% of the wind speed, but at 1 m depth it is only 0.5% of the wind speed. There is, in fact, very little difference in the current at 1 m depth and below, for the two different spectral tails.

The possibility that the wave field affects the drag coefficient is considered in the simulation presented in Fig. 10, in which the final term in equation (8) is set equal to zero. This means that the total surface stress from the atmosphere to the ocean is increased above the nominal wind stress,  $\tau$ , by an amount sufficient to allow the waves to grow without reducing the direct momentum flux from the wind to the (quasi-Eulerian) current. The waves, in effect “suck up” an extra amount of momentum from the atmosphere, and this is in turn fed back into the current at greater depths via wave dissipation. The resultant effect is to increase the current significantly – the mean surface drift current is increased to over 6% of the wind speed, and the current lower down is increased in proportion.

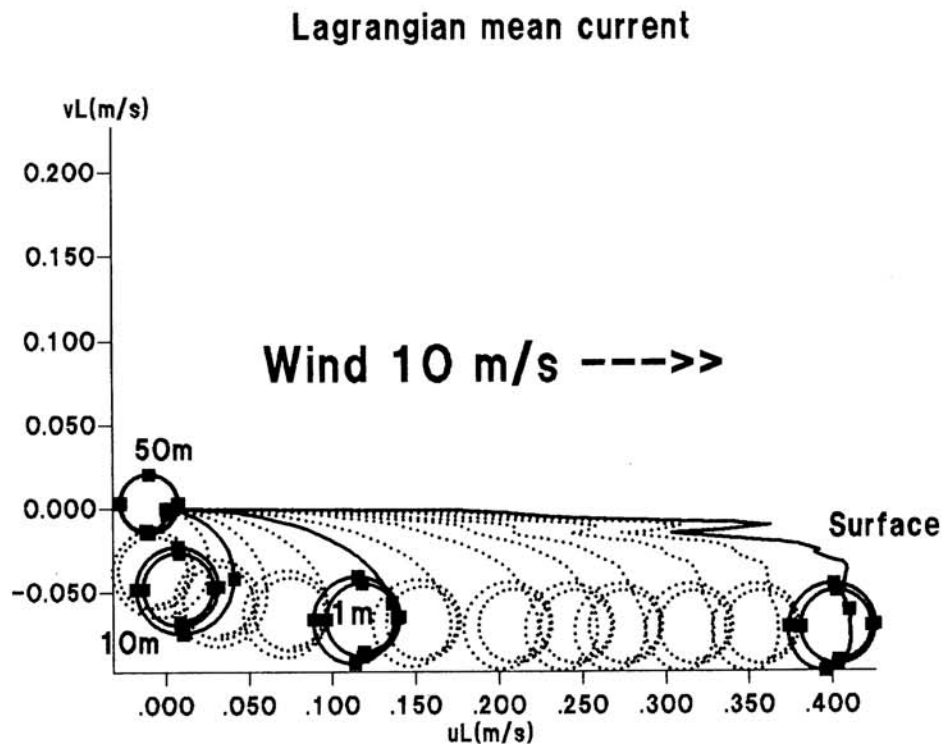


Fig. 3 Hodograph of the Lagrangian mean current, at the surface and depths (–c) of 1 cm, 2 cm, 5 cm, 10 cm, 50 cm, 1 m, 2 m, 5 m, 10 m, 20 m and 50 m. The squares mark each 3 pendulum hours (12 pendulum hours = 14.42 h)

### Quasi-Eulerian current

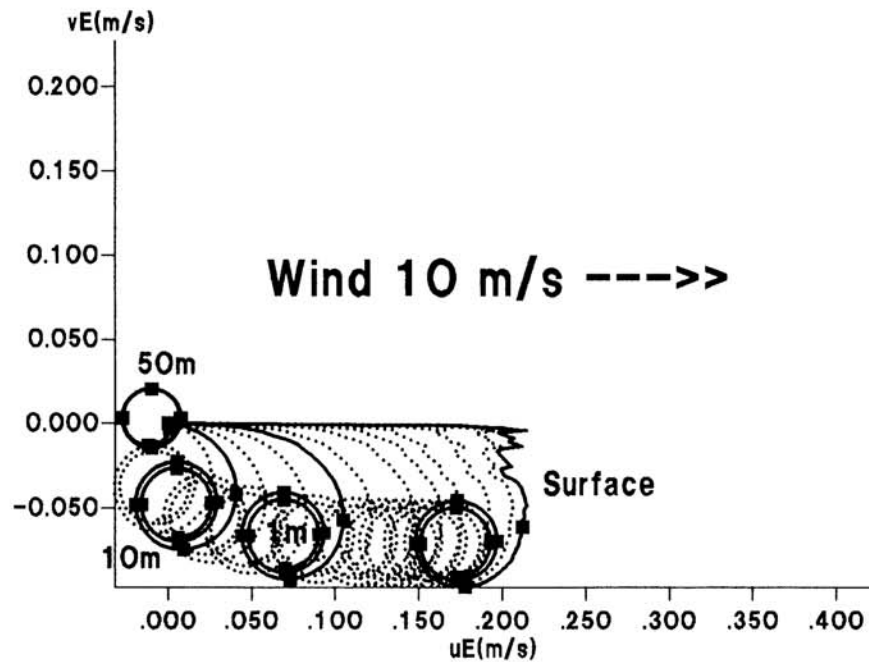


Fig. 4 Hodograph of the quasi-Eulerian current, for the same depths as in Fig. 3.  
The squares mark each 3 pendulum hours

### Lagrangian mean current

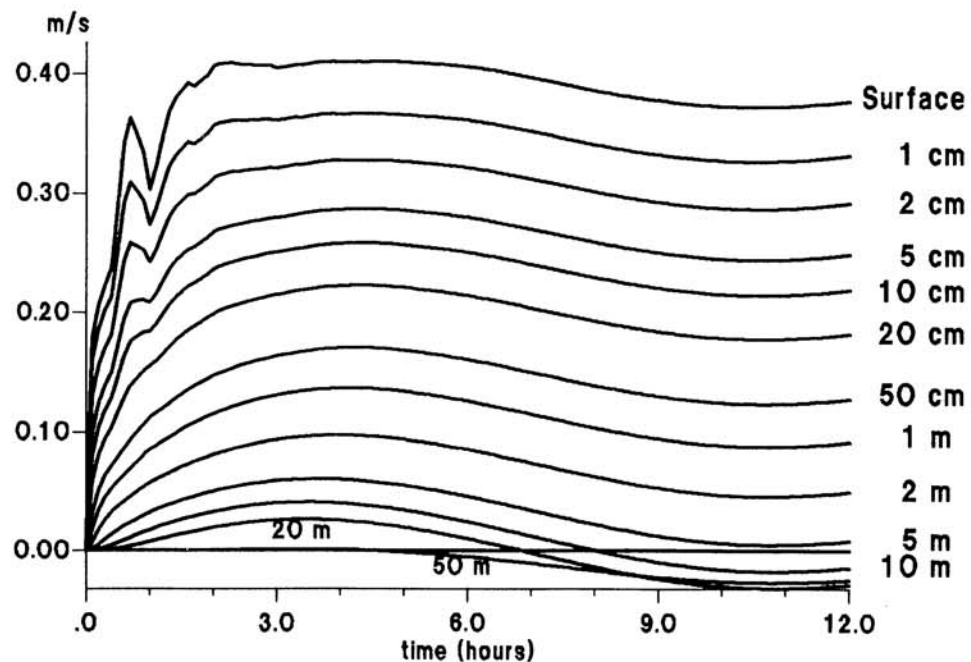


Fig. 5 Time series of the  $x$ -component of the Lagrangian mean current in the upper 50 metres, for the first 12 hours

### Quasi-Eulerian current

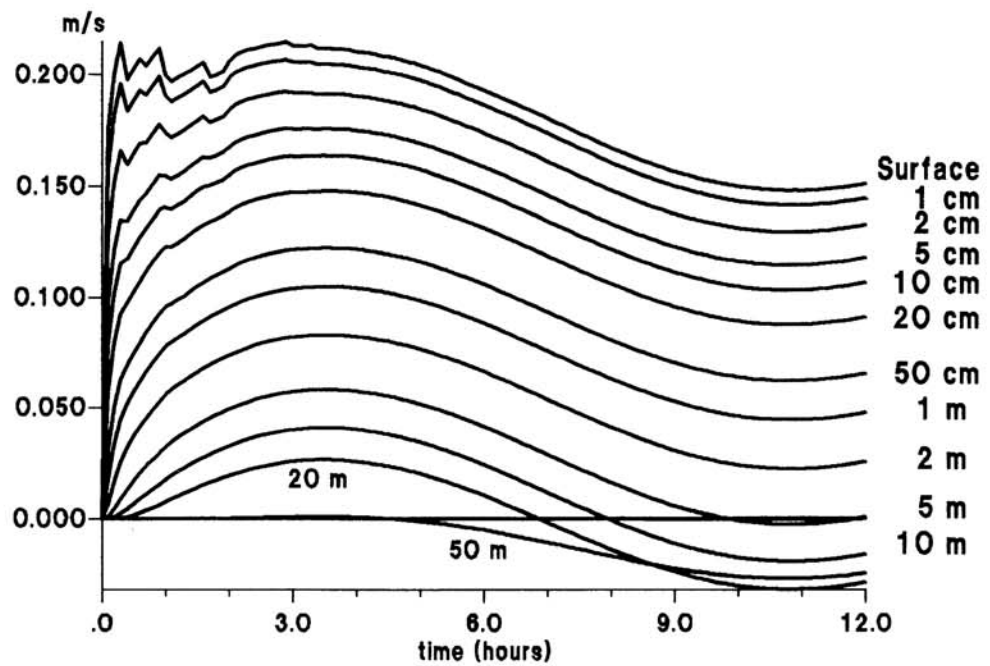


Fig. 6 Time series of the  $x$ -component of the quasi-Eulerian current in the upper 50 metres, for the first 12 hours. Note that the scale is not the same as in Fig. 5

### No waves

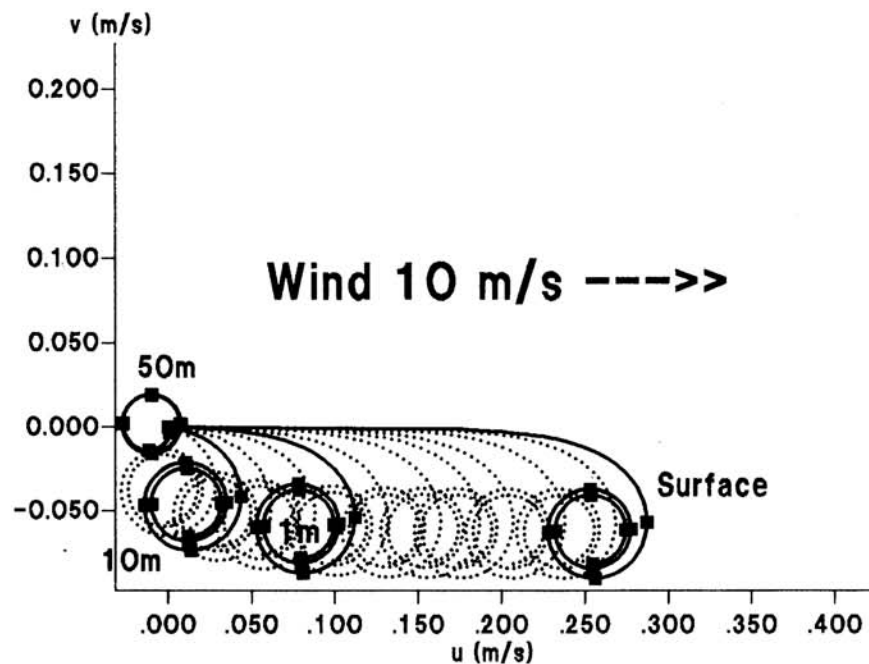


Fig. 7 Hodograph of the current simulated assuming no surface waves, for the same depths as Fig. 3. The squares mark each 3 pendulum hours



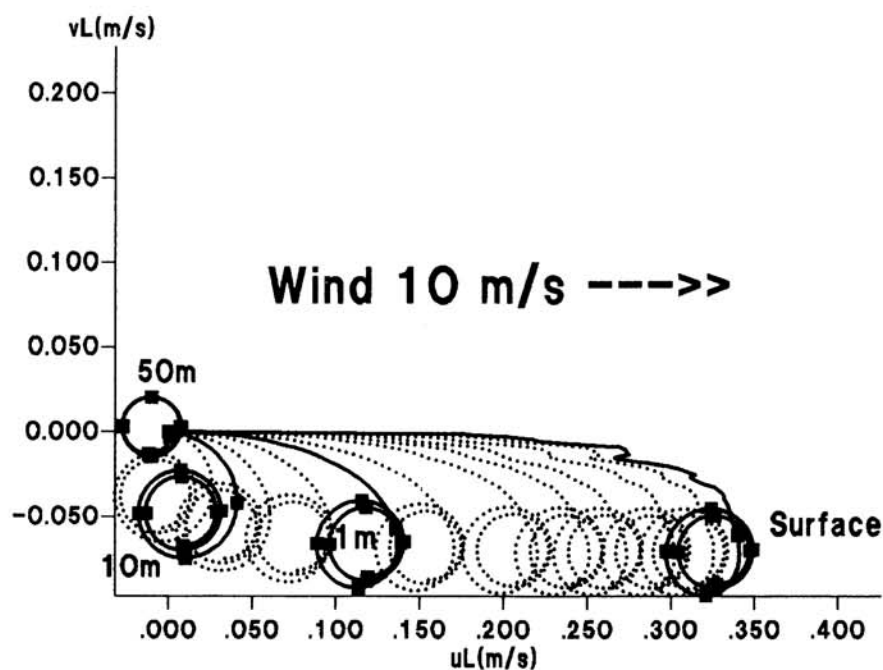
**$f^{*-5}$  spectral tail**

Fig. 8 Hodograph of the current simulated assuming a wave spectral tail proportional to  $f^{-5}$ , instead of  $f^{-4}$ . Depths the same as in Fig. 3. The squares mark each 3 pendulum hours

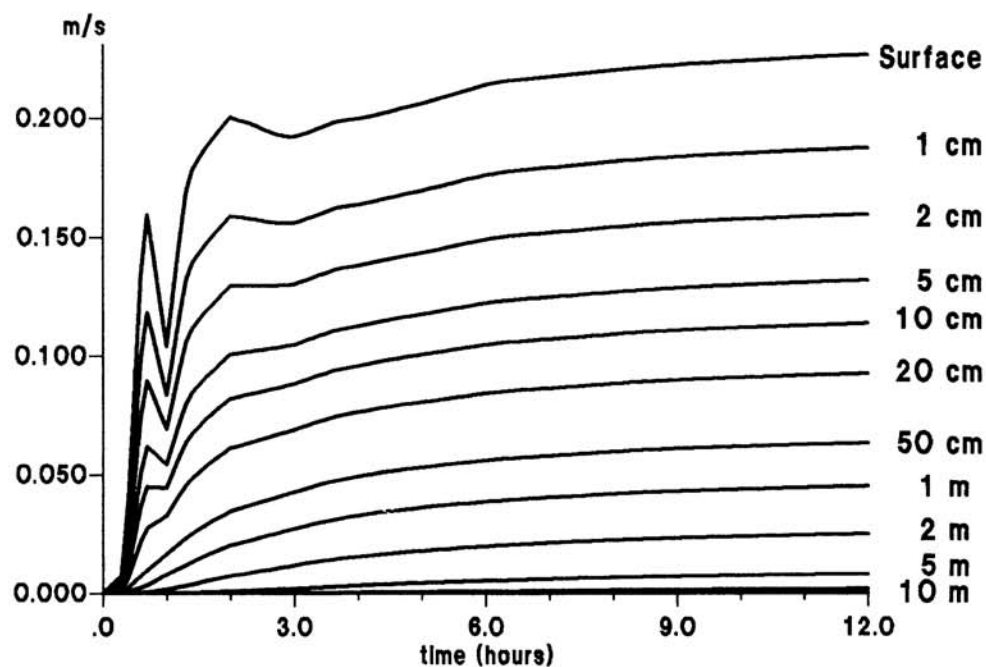
**Stokes drift**

Fig. 9 Time series of the Stokes drift, which is directed along the  $x$ -axis, for the first 12 hours ( $f^{-4}$  spectral tail)

### Enhanced surface stress

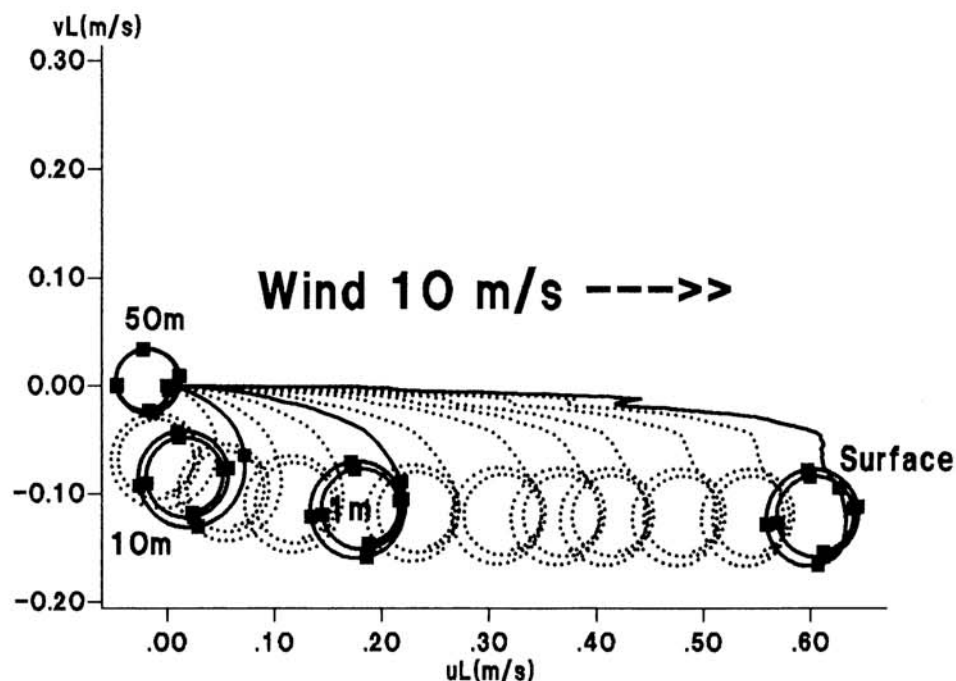


Fig. 10 Hodograph of the current simulated with a wave-enhanced surface stress, for the same depths and the same wave field as in Fig. 3. The squares mark each 3 pendulum hours. Note that the scale is not the same as in Fig. 3

### Significant wave height $H_{m0} = 4 \sqrt{E}$

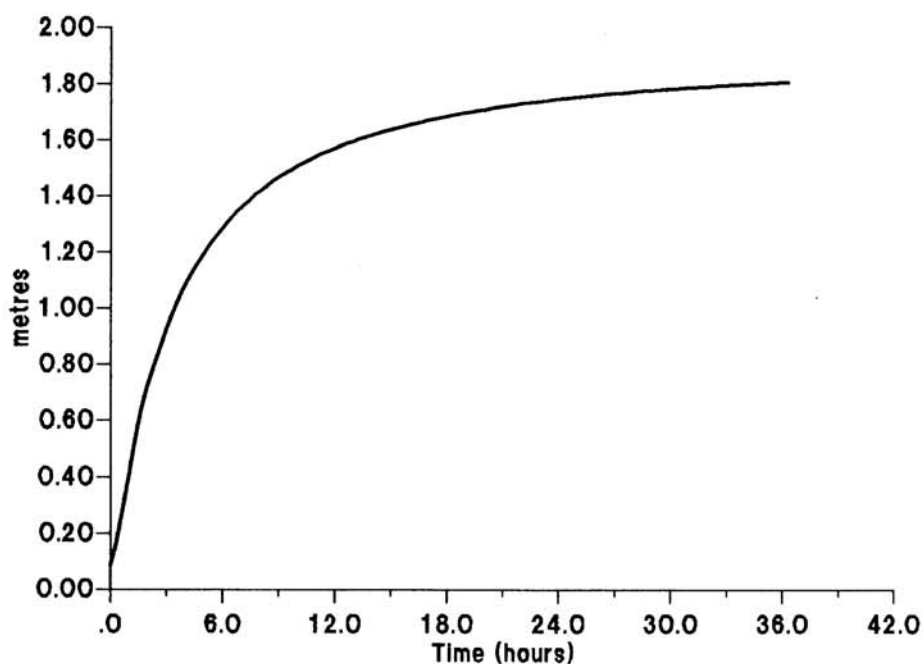


Fig. 11 Time series of the significant wave height calculated by the wave model. (Wind speed  $10 \text{ m} \cdot \text{s}^{-1}$  for  $t > 0$ .)

In all the simulations here presented, apart from the one in which the effect of waves is ignored, the current exhibits rapid oscillations during the first 2 to 3 hours. This is probably due to an oscillatory response of the wave model to the sudden onset of the wind at  $t = 0$ . Although the total wave energy, represented in Fig. 11 by the significant wave height,  $H_{m0} = 4 (E[\zeta^2]_{c=0})^{1/2}$ , does not show any oscillations, the oscillations show up in the time series of the Stokes drift in the upper 0.5 m. Although the effect may be physical, it may also be due to some kind of instability in the wave model – the integration technique used in the wave model is partially implicit, but not fully implicit, and the rapid response of the high-frequency part of the wave spectrum may cause some instability (The SWAMP Group [1985], p. 16). In any case, the oscillations in the Stokes drift cannot be a result of the parameterization (9) for  $S_{nl}(f, \theta)$ ,  $f > f_{bm}$ , which is not used at all by the wave model itself.

## 6 Conclusion

The model here presented is a first attempt at combining a wave prediction model and a hydrodynamic model in order to predict near-surface currents. The balance of momentum in the wave field is dealt with by applying a second-order perturbation expansion in a Lagrangian coordinate system, and vertical momentum transport within the current field is by means of a vertically varying eddy viscosity with a maximum value at 12 m depth (for a wind speed of  $10 \text{ m s}^{-1}$ ).

The model gives results which are in reasonable accord with what is known, theoretically and experimentally, about the behaviour of the current in the near-surface Ekman layer. The results within the upper 1 m are sensitive to the details of the high-frequency tail of the wave spectrum, and to the behaviour of the surface stress (its dependence on the wave field, for example).

There are, however, some points which need further study. It has not been possible to use the eddy viscosity which acts on the current to damp out the waves, as was suggested by Weber [1983 a, b], and an empirical vertical profile of the wave-current momentum flux has had to be used (the function  $N(f, \theta; c)$  in equation (7)). The 3G-WAM wave model, when forced by a rapidly varying wind stress, produces oscillations in the high-frequency part of the spectrum which are reproduced in the Stokes drift – more investigations of the wave model behaviour are required, either to justify or to eliminate them. Since high-frequency components give significant contributions to wave momentum, the tail of the wave spectrum is important, and better results may be obtained by modelling the spectral tail directly, rather than just extrapolating a frequency power-law. There is a need for improved theoretical and experimental studies of hydrodynamic processes in both the atmospheric and oceanic boundary layers: examples are wave growth parameterization and Langmuir circulations, which are obviously affected by wind-wave and wave-wave interaction and which significantly influence the effective vertical eddy viscosity.

## Acknowledgements

I would like to thank Johannes Guddal, Anne Karin Magnusson and Magnar Reistad, of the Norwegian Meteorological Institute (DNMI), and also, of course, the WAM group, for making the 3G-WAM model available to the cooperative project “Model studies of Norwegian coastal waters”, whose participants include DNMI and the Bergen Scientific Centre.

## References

- Andrews, D. G. and M. E. McIntyre, 1978: An exact theory of nonlinear waves on a Lagrangian-mean flow. *J. Fluid Mech.* **89**, 609–646.
- Backhaus, J. O., 1985: A three-dimensional model for the simulation of shelf sea dynamics. *Dt. hydrogr. Z.* **38**, 165–187.
- Barstow, S. F. and H. E. Krogstad, 1984: General analysis of directional ocean wave data from heave/pitch/roll buoys. *Modeling, Identification and Control* **5**, 47–70.
- Davies, A. M., 1986: Application of a spectral model to the calculation of wind drift currents in an idealized sea. *Contin. Shelf Res.* **5**, 579–610.
- Davies, A. M. and J. E. Jones, 1987: Modelling turbulence in shallow sea regions. In: *Small-scale turbulence and mixing in the ocean*. (Eds. J. C. J. Nihoul and B. M. Jarmart) Amsterdam: Elsevier (Proc. 19th Liège Colloquium on Ocean Hydrodynamics), p. 63–76.
- Ekmann, V. W., 1905: On the influence of the Earth's rotation on ocean-currents. *Arkiv för Matematik, Astronomi och Fysik* **2**, No. 11, 1–52.
- Gerstner F. J., 1804: *Theorie der Wellen*. Abhandl. Kgl. Böhm. Ges. Wiss., Prague.
- Gill, A. E., 1982: *Atmosphere-Ocean Dynamics*. London: Academic Press, 662 p. (International Geophysics Series, Vol. 30.)
- Gjevik, B., H. E. Krogstad, A. Lygre and O. Rygg, 1988: Long-period swell wave events on the Norwegian shelf. *J. phys. Oceanogr.* **18**, 724–737.
- Hasselmann, K., 1962: On the non-linear energy transfer in a gravity-wave spectrum. Part 1. General theory. *J. Fluid Mech.* **12**, 481–500.
- Hasselmann, K., 1970: Wave-driven inertial oscillations. *Geophys. Fluid Dyn.* **1**, 463–502.
- Hasselmann, S., K. F. Hasselmann, J. H. Allender and T. P. Barnett, 1985: Computations and parameterizations of the nonlinear energy transfer in a gravity-wave spectrum. Part II: Parameterizations of the nonlinear energy transfer for application in wave models. *J. phys. Oceanogr.* **15**, 1378–1391.
- Huang, N. E., 1979: On surface drift currents in the ocean. *J. Fluid Mech.* **91**, 191–208.
- Jenkins, A. D., 1986: A theory for steady and variable wind- and wave-induced currents. *J. phys. Oceanogr.* **16**, 1370–1377.
- Jenkins, A. D., 1987a: Wind and wave induced currents in a rotating sea with depth-varying eddy viscosity. *J. phys. Oceanogr.* **17**, 938–951.
- Jenkins, A. D., 1987b: A Lagrangian model for wind- and wave-induced near-surface currents. *Coastal Engng* **11**, 513–526.
- Jenkins, A. D., 1987c: A dynamically consistent model for simulating near-surface ocean currents in the presence of waves. *Advances in Underwater Technology, Ocean Science and Offshore Engineering, Volume 12: Modelling the Offshore Environment*. London: Graham and Trotman for the Society for Underwater Technology, p. 343–352.
- Kitajgorodskij, S. A., 1973: *The physics of air-sea interaction*. English translation. Jerusalem: Israel Program for Scientific Translations, 237 p.
- Komen, G. J., S. Hasselmann and K. F. Hasselmann, 1984: On the existence of a fully developed wind-sea spectrum. *J. phys. Oceanogr.* **14**, 1271–1285.
- Leibovich, S. and S. Paolucci, 1981: The instability of the ocean to Langmuir circulations. *J. Fluid Mech.* **102**, 141–167.
- Longuet-Higgins, M. S., 1953: Mass transport in water waves. *Philos. Trans. Roy. Soc., London (A)* **245**, 535–581.
- Longuet-Higgins, M. S., 1970: Longshore currents generated by obliquely incident sea waves, 1. *J. geophys. Res.* **75**, 6778–6789.
- McIntyre, M. E., 1981: On the 'wave momentum' myth. *J. Fluid Mech.* **106**, 331–347.
- Madsen, O. S., 1977: A realistic model of the wind-induced Ekman boundary layer. *J. phys. Oceanogr.* **7**, 248–255.
- Pollard, R. T., 1970: Surface waves with rotation: An exact solution. *J. geophys. Res.* **75**, 5895–5898.
- Roache, P. J., 1972: *Computational Fluid Dynamics*. Albuquerque, New Mexico: Hermosa Publ., 446 p.
- Snodgrass, F. E., G. W. Groves, K. F. Hasselmann, G. R. Miller, W. H. Munk and W. H. Powers, 1966: Propagation of ocean swell across the Pacific. *Philos. Trans. Roy. Soc. London (A)* **259**, 431–497.
- Stokes, G. G., 1847: On the theory of oscillatory waves. *Trans. Cambridge philos. Soc.* **8**, 441–455.
- The SWAMP Group, 1985: *Sea Wave Modeling Project (SWAMP). Part I: Principal results and conclusions*. Ocean Wave Modeling. New York: Plenum Press, p. 1–153.
- Thorpe, S. A., 1985: Small-scale processes in the upper ocean boundary layer. *Nature* **318**, 519–522.
- Ursell, F., 1950: On the theoretical form of ocean swell on a rotating earth. *Mon. Not. Roy. astron. Soc. (Geophys. Suppl.)* **6**, 1–8.



- The WAMDI Group (S. Hasselmann, K. F. Hasselmann, E. Bauer, P. A. E. M. Janssen, G. J. Komen, L. Bertotti, P. Lionello, A. Guillaume, V. C. Cardone, J. A. Greenwood, M. Reistad, L. Zambresky and J. A. Ewing), 1988: The WAM model – a third generation ocean wave prediction model. *J. phys. Oceanogr.* **18**, 1775–1810.
- Weber, J. E., 1981: Ekman currents and mixing due to surface gravity waves. *J. phys. Oceanogr.* **11**, 1431–1435.
- Weber, J. E., 1983a: Steady wind- and wave-induced currents in the open ocean. *J. phys. Oceanogr.* **13**, 524–530.
- Weber, J. E., 1983b: Attenuated wave-induced drift in a viscous rotating ocean. *J. Fluid Mech.* **137**, 115–129.
- Wolf, J., K. P. Hubbert and R. A. Flather, 1988: A feasibility study for the development of a joint surge and wave model. Proudman Oceanogr. Laboratory, Report No. 1, 109 p.

Eingegangen am 15. Dezember 1988

Angenommen am 1. August 1989

Anschrift des Verfassers:

Dr. Alastair D. Jenkins

Bergen Scientific Centre, IBM, Thormøhlensgate 55, N-5008 Bergen, Norwegen